An analytical model for the wettability switching characteristic of a nanostructured thermoresponsive surface

Ghanashyam Londe,[1] Anindarupa Chunder,[2] Lei Zhai,[2] and Hyoung J. Cho[3,a)]
[1]*Department of Electrical Engineering, University of Central Florida, Orlando, Florida 32816-2450, USA*
[2]*Department of Chemistry and Nanoscience Technology Center, University of Central Florida, Orlando, Florida 32826-3271, USA*
[3]*Department of Mechanical, Materials and Aerospace Engineering, University of Central Florida, Orlando, Florida 32816-2450, USA*

(Received 4 September 2008; accepted 25 January 2009; published online 23 April 2009)

The applications of thermoresponsive surfaces require the development of a rigorous mathematical treatment for these surfaces to understand and improve their behavior. We propose an analytical model to describe the transfer characteristics (variation in contact angle versus temperature) of a unique nanostructured thermosensitive surface, consisting of silica nanoparticles and a hydrophilic/hydrophobic thermoresponsive polymer, poly(*N*-isopropylacrylamide). Three different thermosensitive platforms were fabricated and the contact angle change of a water droplet on the surface with varying surface temperature was analytically modeled. © *2009 American Institute of Physics*. [DOI: 10.1063/1.3103270]

Surfaces that change their wettability with varying temperature have drawn considerable attention as their hydrophobicity can be finely tuned over a wide range of stimuli. These surfaces have a variety of applications including microflow regulation,[1] force transduction,[2] drug delivery,[3] and molecular filtering.[4]

Poly(*N*-isopropylacrylamide) (PNIPAAm) is a well known polymer that is sensitive to changes in the ambient heat and has a lower critical solution temperature (LCST) range of about 28–33 °C. The polymer chains hydrate and stay in extended structures when the solution temperature is below the LCST range, giving rise to hydrophilic structures. In contrast, the polymer chains form intramolecular hydrogen bonds and dehydrate when the solution temperature increases above the LCST range, resulting in compact hydrophobic structures. PNIPAAm can be grafted on a rough surface to create surface that can switch from superhydrophobicity to superhydrophilicity by varying the ambient temperature.[5] However, an exhaustive mathematical analysis of this unique thermosensitive phenomenon has not been reported as yet.

The hydrophobicity of a surface depends on its surface energy and roughness. The energy of a surface is determined by the surface functional groups. The effect of roughness on hydrophobicity has been described by the Wenzel model[6] and the Cassie model.[7] Based on these models, previous studies suggested that small scale (nanoscale) features with a larger scale spacing (microscale) would yield better hydrophobic characteristics.[8,9] Accordingly, a multilayered polyelectrolyte surface decorated with silica nanoparticles and functionalized with a low surface energy material could be fabricated to realize superhydrophobic surface.[10] Layer-by-layer deposition technique was used to build uniform and conformal multilayer films of poly(allylamine hydrochloride) (PAH) and silica nanoparticles with a precise control of film thickness and roughness. The porous polyelectrolyte multilayers give rise to roughness on the micron scale and the silica nanoparticles give roughness at the nanoscale. The surface was further functionalized with PNIPAAm. Three different kinds of thermoresponsive surfaces, fabricated on glass slides are described in Table I. Surface C was finally functionalized with a very thin layer of a low surface energy material, (1*H*, 1*H*, 2*H*, 2*H*-perfluorooctyl) silane (perfluorosilane).

The switching characteristics depicting the variation in contact angle versus temperature are shown in Figs. 1(a)–1(c) for each type of surface. Surface C shows a higher maximum and minimum contact angle than surface B at the maximum and minimum operating temperatures, respectively. This is due to the inherent higher average surface roughness of surface C.

The switching characteristic can be modeled on a standard logistic function,

$$Y(x) = \frac{1}{1 + e^{-kx}}, \tag{1}$$

where k is the transition slope factor of the function.

Logistic functions to describe various phenomenon have been reported by others.[11,12] We have developed a modified logistic function to fit the ordinate and abscissa values; transition and saturation slope; surface roughness and the LCST of the polymer. The equation for the contact angle of a water droplet (θ) can be given by

$$\theta(T) = \theta_{\min} + \frac{\beta + \phi_{\text{sat}}}{1 + e^{-k(T - T_{\text{LCS}})}}, \tag{2}$$

where T is the operating temperature, $\theta_{\min}$ is the contact angle at room temperature, β is the magnitude compensation factor, ϕ_{sat} is the saturation slope factor, and T_{LCS} is the absolute lower critical solution temperature of the thermosensitive polymer. The curve given by Eq. (2) can be divided into two regions, namely, the linear and the saturation region. The linear region spans the LCST range and exhibits maximum gain.

Figures 2(a)–2(c) show the theoretical curve fitted on to the experimental curve of surfaces A, B, and C, respectively.

a)Electronic mail: joecho@mail.ucf.edu.

TABLE I. The three types of thermoresponsive surfaces fabricated with different surface roughness.

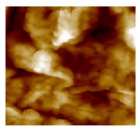 Surface A: Intermediate surface roughness	PNIPAAm was grafted from the surface and partially covered the surface, retaining the surface roughness as confirmed by the atomic force microscope (AFM) image.
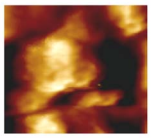 Surface B: Low surface roughness	PNIPAAm was grafted from the surface, fully covered the surface, and filled the pores, greatly reducing the surface roughness.
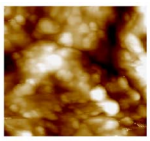 Surface C: High surface roughness	Silica nanoparticles were deposited on surface B to partially cover the surface, regenerating the surface roughness.

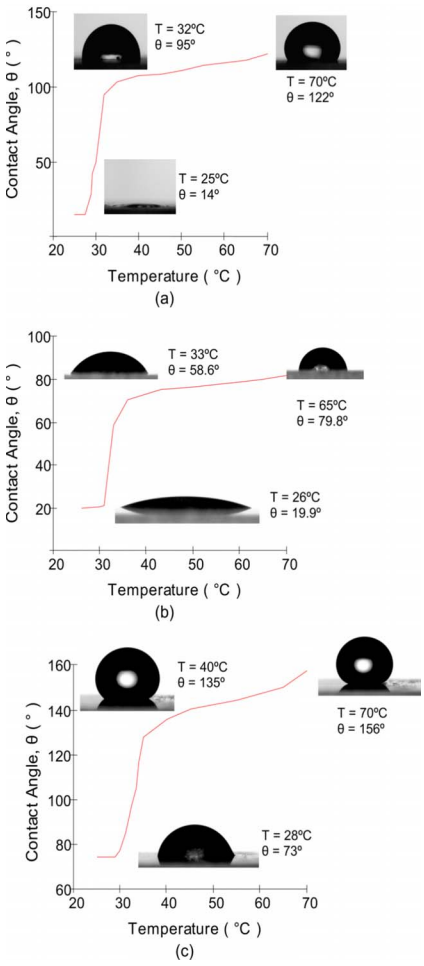

FIG. 1. (Color online) [(a)–(c)] Plot of contact angle vs surface temperature for surfaces A, B, and C, respectively. Inset: Optical micrographs of the water droplet at low, medium, and high temperatures.

The proposed model is valid from ambient temperatures—through the LCST range of PNIPAAm—until the temperature reaches a high value ($\geq$70 °C) at which the water droplet becomes unstable and evaporates. In the actual experiments, we found that the hydrophilic to hydrophobic switching takes place over a small range of LCSTs and that T_{LCS} (reported in the literature) is approximately at the midpoint of this LCST range. The contact angle of a water droplet on a PNIPAAm switching surface exponentially increases as the surface temperature increments through the LCST range. As long as $\mathrm{LCST}_{\mathrm{min}} \leq T \leq \mathrm{LCST}_{\mathrm{max}}$, the exponential term in the denominator of Eq. (2) dominates, giving rise to a steep slope in the linear region of the transfer characteristic (Fig. 2). The contact angle increases over a range of LCSTs as the PNIPAAm molecules require time to change their conformation from hydrophilic to hydrophobic.

The change in contact angle in the linear region (Fig. 2) depends on the thickness of PNIPAAm grafted on the surface. The slope of the Eq. (2) in the linear region is directly proportional to the transition slope factor k. Hence, we can model "surface B" (which has a thicker layer of PNIPAAm on the surface) with a higher value of k compared to the other surfaces.

As the temperature is increased beyond the linear region, the gain in hydrophobicity becomes minimal and gives rise to the slope in the saturation region. In the saturation region, the water droplet is subjected to competing forces. The droplet absorbs heat energy of the test sample on which it is placed, resulting in a decrease of the surface energy of the water droplet. On the other hand, the hydrophobic nature of the thermosensitive polymer and the roughness of the sample tend to increase the surface energy of the water droplet. The saturation slope which is proportional to the operating temperature T, can be modeled to the measured transfer characteristic by using the saturation slope factor $\phi_{\mathrm{sat}}(T) = T/C_{\mathrm{slp}}$, where C_{slp} is a process dependent fitting parameter. The exact relation between the saturation slope (i.e., the extent of hydrophobicity) and C_{slp} needs to be further investigated.

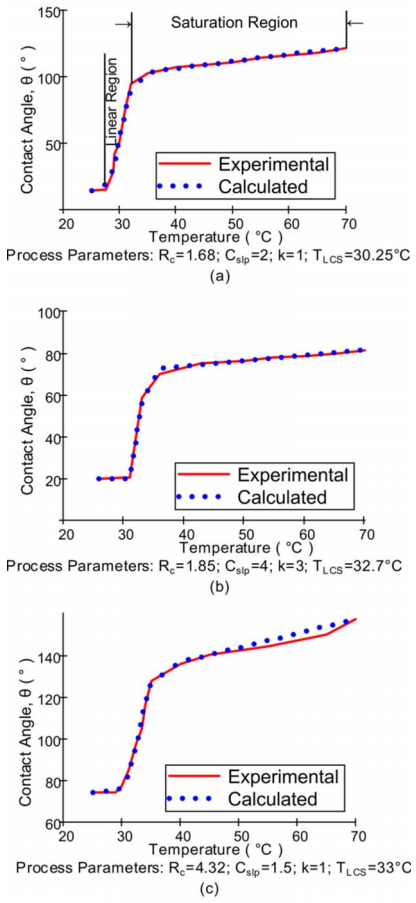

FIG. 2. (Color online) [(a)–(c)] Plot of the calculated contact angle fitted on the measured contact angle vs surface temperature for surfaces A, B, and C, respectively.

The magnitude of the transfer characteristic which is proportional to the maximum contact angle θ_{max} (measured at the highest operating temperature), can be accurately modeled by using the magnitude compensation factor $\beta = \theta_{max}/R_C$. R_C is a process dependent fitting parameter.

We use the switching characteristic of surface A for further mathematical analysis. The first differential of Eq. (2) is given by

$$m(T) = \frac{e^{k(T-T_{LCS})} + k(T+\beta C_{slp}) + 1}{4C_{slp}\cosh\left[\frac{k(T-T_{LCS})}{2}\right]^2}. \quad (3)$$

The maximum gain (i.e., the maximum value of m) of the contact angle occurs at the T_{LCS}.

The defining metric of a thermoresponsive polymer is the onset and end temperatures of the LCST range. These temperatures can be calculated by using the piece-wise linear approximation approach. The linear region of the transfer function given by Eq. (2) can be represented by a straight line which intersects an upper (A_u) and a lower ($A_l = \theta_{min}$) bound. The boundaries are defined over a contact angle range ($\theta_{range} = A_u - A_l$), such that $\theta_{LCS} = \theta_{min} + \theta_{range}/2$, as shown in Fig. 3. θ_{LCS} is the contact angle of the water droplet at T_{LCS}. The onset of the LCST range, characterized by the threshold temperature (T_{thr}) and the end of the LCST range characterized by the saturation temperature (T_{sat}), corresponds to the points where the straight line intersects with the lower and

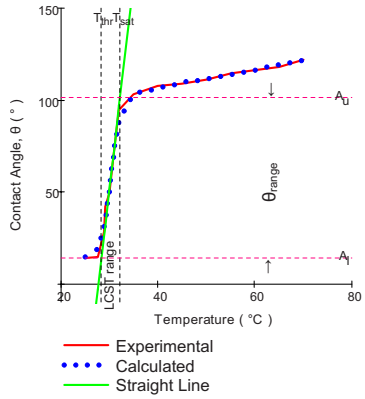

FIG. 3. (Color online) Piece-wise linear approximation method to find the threshold (T_{thr}=28.27 °C) and saturation (T_{sat}=32.23 °C) temperatures to characterize the onset and end of the LCST range. The contact angle at T_{thr} is θ_{thr}=24.73° and at T_{sat} is θ_{sat}=92.04°.

upper bounds, respectively. T_{thr} and T_{sat} are the temperatures at which the value of the contact angles are approximately 10% above and below A_l and A_u, respectively.

Substituting the value of m at T_{LCS} [from Eq. (3)] and the value of the constant C (for the condition $y = \theta_{min} + \theta_{range}/2$ at $x = T_{LCS}$) in the equation of the straight line $y = mx + C$, we derive an expression for the linear region of the transfer function as

$$\theta(T) = \frac{2 + k(T_{LCS} + \beta C_{slp})}{4C_{slp}} T + \theta_{min} + \frac{\theta_{range}}{2} - \frac{T_{LCS}[k(T_{LCS} + \beta C_{slp}) + 2]}{4C_{slp}}. \quad (4)$$

Solving for the value of T_{thr} at $\theta = A_l$, we get

$$T_{thr} = T_{LCS} - \frac{2C_{slp}\theta_{range}}{T_{LCS}k + \beta k C_{slp} + 2}. \quad (5)$$

Similarly, the value of T_{sat} at $\theta = A_u$ is

$$T_{sat} = T_{LCS} + \frac{2C_{slp}\theta_{range}}{T_{LCS}k + \beta k C_{slp} + 2}. \quad (6)$$

The proposed model, analysis, and expressions provide a broad mathematical framework for thermoresponsive surfaces that exhibit a sigmoidal logistic transfer characteristic.

This work has been supported by National Science Foundation (EEC0741508, ECS0348603, DMR0746499).

[1]G. Londe, A. Chunder, A. Wesser, L. Zhai, and H. J. Cho, Sens. Actuators B **132**, 431 (2008).
[2]J. Xi, J. J. Schmidt, and C. D. Montemagno, Nature Mater. **4**, 180 (2005).
[3]D. Kuckling, C. D. Vo, and S. E. Wohlrab, Langmuir **18**, 4263 (2002).
[4]G. V. Rama Rao, M. E. Krug, S. Balamurugan, H. Xu, Q. Xu, and G. P. Lopez, Chem. Mater. **14**, 5075 (2002).
[5]T. Sun, G. Wang, L. Feng, B. Liu, Y. Ma, L. Jiang, and D. Zhu, Angew. Chem., Int. Ed. **43**, 357 (2004).
[6]R. N. Wenzel, Ind. Eng. Chem. **28**, 988 (1936).
[7]A. B. D. Cassie and S. Baxter, Trans. Faraday Soc. **40**, 546 (1944).
[8]J. Bico, C. Marzolin, and D. Qu, Europhys. Lett. **47**, 220 (1999).
[9]N. A. Patankar, Langmuir **19**, 1249 (2003).
[10]L. Zhai, F. C. Cebeci, R. E. Cohen, and M. F. Rubner, Nano Lett. **4**, 1349 (2004).
[11]L. M. McDowall and R. A. L. Dampney, Am. J. Physiol. Heart Circ. Physiol. **291**, H2003 (2006).
[12]D. Pignon, P. J. M. Parmiter, J. K. Slack, M. A. Hands, T. J. Hall, M. Daalen, and J. Shawe-Taylor, Opt. Lett. **21**, 222 (1996).